Synchrotron Speciation of Silver and Zinc Oxide Nanoparticles Aged in a Kaolin Suspension

ARTICLE *in* ENVIRONMENTAL SCIENCE AND TECHNOLOGY · FEBRUARY 2010

Impact Factor: 5.33 · DOI: 10.1021/es9032265 · Source: PubMed

5 AUTHORS, INCLUDING:

Kirk G Scheckel
United States Environmental Protection A…
147 PUBLICATIONS **3,887** CITATIONS

SEE PROFILE

Todd P Luxton
United States Environmental Protection A…
32 PUBLICATIONS **999** CITATIONS

SEE PROFILE

Amro M El Badawy
University of Cincinnati
21 PUBLICATIONS **990** CITATIONS

SEE PROFILE

Synchrotron Speciation of Silver and Zinc Oxide Nanoparticles Aged in a Kaolin Suspension

KIRK G. SCHECKEL,*,† TODD P. LUXTON,† AMRO M. EL BADAWY,‡ CHRISTOPHER A. IMPELLITTERI,† AND THABET M. TOLAYMAT†

U.S. Environmental Protection Agency, Office of Research and Development, Cincinnati, OH, and Department of Civil and Environmental Engineering, University of Cincinnati, Cincinnati, OH

Received October 22, 2009. Revised manuscript received December 17, 2009. Accepted December 21, 2009.

Assessments of the environmental fate and mobility of nanoparticles must consider the behavior of nanoparticles in relevant environmental systems that may result in speciation changes over time. Environmental conditions may act on nanoparticles to change their size, shape, and surface chemistry. Changing these basic characteristics of nanoparticles may result in a final reaction product that is significantly different than the initial nanomaterial. As such, basing long-term risk and toxicity on the initial properties of a nanomaterial may lead to erroneous conclusions if nanoparticles change upon release to the environment.

The influence of aging on the speciation and chemical stability of silver and zinc oxide nanoparticles in kaolin suspensions was examined in batch reactors for up to 18 months. Silver nanoparticles remained unchanged in sodium nitrate suspensions; however, silver chloride was identified with the metallic silver nanoparticles in sodium chloride suspensions and may be attributed to an in situ silver chloride surface coating. Zinc oxide nanoparticles were rapidly converted via destabilization/dissolution mechanisms to Zn^{2+} inner-sphere sorption complexes within 1 day of reaction and these sorption complexes were maintained through the 12 month aging processes. Chemical and physical alteration of nanomaterials in the environment must be examined to understand fate, mobility, and toxicology.

Introduction

Manufactured nanoparticles such as zerovalent metal and metal oxide nanoparticles are used in a wide range of applications such as electronics, pharmaceuticals, antimicrobial commercial products, environmental remediation, catalysis, and material sciences (*1*−*4*). As the use and production of nanoparticles increases, there is a greater likelihood for release into the environment (*2, 5*−*7*). Size, shape, and surface charge are some of several factors that govern the colloidal chemistry of nanoparticles in the environment which may lead to agglomeration and/or transformation (*8, 9*) as residence time increases. For obvious concerns, examining the physical and chemical behavior of released nanomaterials is essential for understanding mobility, determining fate, and predicting possible exposure pathways.

Aging, as physical or chemical transformations over time, is essential for understanding the fate of nanoparticles in the environment. Most aging studies of nanoparticles in the literature assess the surface oxidation of nanoscale zerovalent iron (nZVI) (*9*−*13*). The study of aging is vital in the case of nZVI, which has environmental remediation applications, since the transformations might indicate less reactivity with time (*14*) Nonetheless, research on the aging and transformation of other metal (oxide) nanoparticles has been scarce. Since elemental speciation is directly linked to bioavailability and toxicity, phase identification is useful in predicting adverse effects (*15*). Phenrat et al. (*16*) examined the neurotoxicity of fresh and aged (>11 months) nZVI with cultured rodent microglia (BV2) and neurons (N27). Oxidative stress was notably higher for the fresh nZVI than the aged nZVI indicating that the oxidized (surface modified) aged nZVI was less toxic (*16*). If nanoparticles change from their original form once introduced to the environment, it is necessary to identify these changes and then determine if the new forms possess different characteristics relative to the original material.

While understanding the aging effects of iron-based nanoparticles is important to maximize the efficiency of remediation, there is a significant data gap regarding aging of other man-made nanoparticles in the environment. Silver nanoparticles are among the most widely used nanomaterials in consumer products as an antimicrobial agent (*2*). Zinc oxide also possesses antimicrobial properties but is most often employed in sunscreens or as a catalyst for methanol synthesis (*17, 18*). Input of silver or zinc oxide nanoparticles into the natural environment through consumer products, industrial activity, or end of life management may cause harm to ecoreceptors as demonstrated in laboratory toxicological tests (*19*−*23*). However, the influence of aging on the long-term chemical stability, fate, and mobility of nanoparticles in the environment interacting with natural reactive surfaces which may alter their reactivity has not been examined in detail.

The objective of this study was to evaluate the aging of silver (Ag) and zinc (Zn) oxide nanomaterials in controlled kaolin suspensions using X-ray absorption spectroscopy to determine if chemical speciation changes occur up to an 18 month reaction period.

Experimental Section

Materials. Kaolin was purchased from Acros Organics (Geel, Belgium) and was Na^+ saturated with excess salts removed by dialysis followed by freeze-drying. Kaolin is a well-characterized dioctahedral phyllosilicate clay mineral with low shrink-swell properties, low cation exchange capacity, and is a common constituent in soils and sediments (*24*). Kaolin particle sizes averaged 25 μm (Mastersizer, Malvern Instruments, Worcestershire, UK). The surface area was 11.5 $m^2\ g^{-1}$ (Micromeritics Gemini, Norcross, GA). Point of zero charge was determined to be approximately 4.5 by potentiometric titration analyses (*25*). X-ray diffraction (XRD) (Panalytical X'Pert, Netherlands) analysis showed a minor impurity of quartz. Elemental analyses (inductively coupled plasma optical emission spectrometry (ICP-OES), Perkin-Elmer 2100 DV, Waltham, MA) following a microwave acid digestion (EPA Method 3051) indicated, other than major amounts of Al and Si, approximately 1000 mg kg^{-1} of iron

* Corresponding author phone: 513-487-2865; fax: 513-569-7879; e-mail: Scheckel.Kirk@epa.gov.
† U.S. Environmental Protection Agency.
‡ University of Cincinnati.

10.1021/es9032265
Published on Web 01/15/2010

TABLE 1. Collected Solids Concentration (mg kg^{-1}) and Standard Deviations of Silver and Zinc Reacted in a Kaolin Suspension for Various Aging Times[a]

aging time	Ag Uncoated w/$NaNO_3$	Ag Organic w/$NaNO_3$	Ag Organic w/NaCl	Sorbed Ag w/$NaNO_3$	ZnO w/$NaNO_3$	Sorbed Zn w/$NaNO_3$
1 hour	–[b]	–	–	–	470 ± 0.62	492 ± 6.05
3 hours	–	–	–	–	483 ± 0.76	502 ± 6.04
6 hours	–	–	–	–	495 ± 2.50	505 ± 3.32
1 day	175 ± 3.58	199 ± 1.43	190 ± 2.20	167 ± 1.27	528 ± 0.44	518 ± 2.81
7 days	206 ± 1.81	206 ± 2.72	217 ± 1.66	209 ± 1.46	–	–
1 months	226 ± 1.21	221 ± 2.05	230 ± 3.27	242 ± 1.71	549 ± 5.41	539 ± 2.46
3 months	249 ± 0.41	226 ± 0.05	244 ± 2.33	258 ± 2.39	–	–
6 months	263 ± 4.49	236 ± 2.16	247 ± 0.40	279 ± 2.09	–	–
12 months	263 ± 2.97	251 ± 1.61	254 ± 0.33	279 ± 2.79	558 ± 2.10	558 ± 1.43
18 months	261 ± 1.70	247 ± 3.34	–	280 ± 2.15	–	–

[a] Maximum possible solids concentrations are 300 mg kg^{-1} for silver and 600 mg kg^{-1} for zinc based on experimental parameters. [b] No data collected.

was present in the kaolin material as primary components. Zinc concentration in the kaolin material was 10.1 mg kg^{-1}, and silver concentration was below detection limit.

Three nanoparticle materials, two silver and one zinc oxide, were employed in this study and purchased from Sigma Aldrich (St. Louis, MO). Each nanomaterial sample was characterized for surface area (Micromeritics Gemini, Norcross, GA) and particle size and surface potential (to determine point of zero charge) (Zetasizer Nano, Malvern Instruments, Worcestershire, UK). One silver nanomaterial, named Ag Organic hereafter, was organically coated with a proprietary compound for dispersion in solvents. It had a particle size of approximately 100 nm, a surface area of 5 m^2 g^{-1}, and a negative surface potential across all pH values. The other silver nanomaterial, named Ag Uncoated hereafter, was a metastable, energetic, activated powder with an average particle size of 148 nm, surface area of 4 m^2 g^{-1}, and a negative surface potential across all pH values. The zinc oxide (ZnO) nanomaterial had a surface area of 23 m^2 g^{-1}, a point of zero charge of about 8.5, and was approximately 100 nm in size.

Kaolin and Nanoparticle Batch Reactions. To investigate the influence of aging on the chemical stability of silver and zinc oxide nanoparticles, kaolin was reacted with the individual nanomaterials in duplicate for periods of 1 hour to 18 months. Experimental conditions included an initial solution concentration of 3 mg L^{-1} silver or 6 mg L^{-1} zinc (from ICP-OES verified stock nanomaterial suspensions of 30 mg L^{-1} silver or 60 mg L^{-1} zinc), 10 g L^{-1} kaolin, and a background electrolyte of 0.01 M $NaNO_3$ or NaCl (for silver nanomaterials only) at pH 6. Sodium chloride was used to evaluate potential silver chloride formation since chloride is ubiquitous in the environment. Sorption of aqueous silver and zinc as nitrate salts were also conducted with the same reaction conditions noted above. The 1 L Teflon reaction vessels containing 0.5 L suspensions (including 50 mL of stock nanomaterial suspension) were purged with N_2 to eliminate CO_2, and the pH was maintained through the addition of 0.1 M NaOH via a Mettler Toledo (Columbus, OH) pH-stat titrator. After 1 week, the reaction vessels were sealed and continuously agitated in a 25 °C incubation environment. At weekly intervals, the suspension pH was checked and readjusted, if necessary, to pH 6 while purging with N_2. At set reaction times, based on preliminary results, from 1 hour to 18 months, 50 mL aliquots of suspension were withdrawn from each reaction vessel and centrifuged at 30 477 g for 10 min (capable of partitioning ≥0.3 μm particles to the collected solids) yielding approximately 0.5 g of solid material. The solids in the centrifuge tube were shock frozen in liquid nitrogen and freeze-dried to stop further aging effects (*26*). Duplicates were homogenized and stored for X-ray absorption spectroscopy (XAS) analysis. Solids concentrations for silver and zinc, from microwave acid digestion and ICP-OES, at various aging times are shown in Table 1.

X-ray Absorption Spectroscopy (XAS). Changes in the chemical speciation of silver or zinc oxide nanoparticles as a function of aging in a kaolin suspension were periodically assessed by XAS to determine information on the nearest-neighbor chemical environment of Ag or Zn such as coordination numbers and interatomic scattering distances. Aging times were chosen based on preliminary research which showed significantly quicker kinetic changes for the ZnO material versus the Ag nanoparticles. Experiments were conducted at the Materials Research Collaborative Access Team's (MRCAT) beamline 10-ID, Sector 10 located at the Advanced Photon Source (APS), Argonne National Laboratory (ANL), Argonne, IL. The electron storage ring operated at 7 GeV in top-up mode. A liquid N_2 cooled double crystal Si(111) monochromator was used to select incident photon energies and a platinum-coated mirror was used for harmonic rejection. The beam energy was calibrated by assigning the first derivative inflection point of the K_α-absorption edge of silver metal (25514 eV) or zinc metal (9659 eV) foils. The samples were prepared as thin pellets with a hand operated IR pellet press and the samples were secured by Kapton tape. The pure nanomaterials and references were diluted with boron nitride to 1000 mg kg^{-1} and formed into pellets. Reference materials presented include bulk ZnO and AgCl from Sigma Aldrich and a Ag metal foil cleaned with a jeweler solution to remove surface impurities. Five XAS spectra were collected in transmission quick-scan mode (0.5 eV steps) at room temperature from −200 to 1000 eV relative to the absorption edge position of Ag or Zn. The I_o chamber was filled with Ar gas for Ag data collection and N_2 for Zn experiments while the I_t detector contained approximately 80:20 Kr:N_2 and 60:40 Ar:N_2 ratios, for Ag and Zn studies, respectively.

The collected spectra were analyzed using the Athena software program in the computer package IFEFFIT (*27*) for data reduction and WinXAS 3.0 (*28*) for data fitting. The five individual spectra for each sample were averaged followed by subtraction of the background through the pre-edge region using the Autobk algorithm (*29*) and normalized to an atomic absorption of one. The data were converted from energy to photoelectron momentum (*k*-space) and weighted by k^3 using WinXAS. Extended X-ray absorption fine structure (EXAFS) spectra were calculated over a typical *k*-space range with a Bessel window. Fourier transforms (FT) were performed to obtain the radial distribution function (RDF) in *R*-space. Plotted *R*-space (Å) data are not phase shift corrected so that the true distances are between 0.3 and 0.5 Å longer than the distances shown. The spectra were fit with FEFF8 ab initio

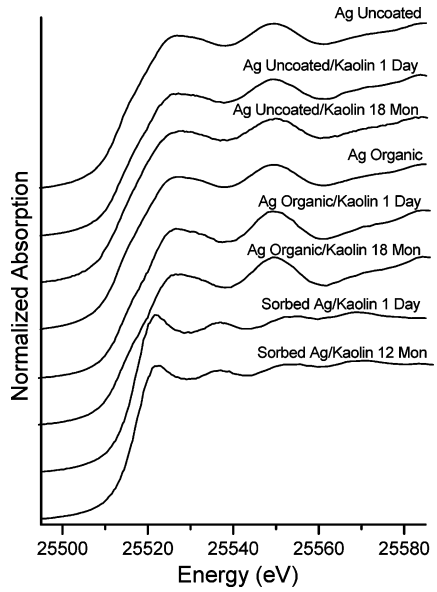

FIGURE 1. Ag−K_α XAS spectra of Ag Uncoated and Ag Organic nanomaterials as pure phases and reacted with kaolin and $Ag(NO_3)_2$ sorption on kaolin as a function of aging time.

calculations to determine phase shift and amplitude functions for single and multiple atomic scattering paths. Structures for Ag metal, AgCl, ZnO, and gahnite ($ZnAl_2O_4$) were used for FEFF8 calculations.

Results and Discussion

X-ray Absorption Near Edge Structure Spectroscopy. The concentration of silver and zinc in the suspension solids after centrifuge separation are noted in Table 1. The rate of silver and zinc nanomaterial retention with the solids was closely in-line with adsorption of aqueous silver and zinc from nitrate salt solutions. While the literature is sparse with data evaluating soil mineral and manufactured nanoparticle interactions (*30, 31*), the surface charge of each material indicates that basic colloid chemistry may contribute to the particle−particle interaction through electrostatic, van der Waals, entropic, and/or steric forces. Colloidal particles can serve as transport vectors in the environment (*32*−*35*). However, one cannot discount that nanoparticles may undergo dissolution mechanisms upon entering the natural environment. The retention of nanoparticles on clay minerals, agglomeration as independent clusters, or dissolution/sorption kinetics may limit nanoparticle mobility in the environment resulting in accumulation in soils or sediments with potential exposure to ecoreceptors.

The reaction of silver and zinc oxide nanoparticles in a kaolin suspension was carried out to evaluate the influence of aging time on chemical speciation and stability of the nanomaterials under relevant environmental conditions in the presence of a common reactive surface. X-ray absorption near edge structure (XANES) spectroscopy data of Ag Uncoated and Ag Organic nanomaterials aged in the kaolin suspension (0.01 M $NaNO_3$) as well as $Ag(NO_3)_2$ sorption to kaolin are shown in Figure 1. Relative to the nonreacted silver nanomaterials (Ag Uncoated and Ag Organic), aging from 1 day to 18 months suggests no change in silver speciation for either nanomaterial (Figure 1) with similar results for data points between these aging periods (data not shown). At pH 6, both the kaolin surface and the silver nanoparticles are negatively charged perhaps limiting direct interaction of the materials. Figure 1 also shows the influence of aging on Ag sorption for the $Ag(NO_3)_2$. The XANES spectra for Ag sorption are distinctly different than the Ag nanomaterials further supporting that Ag nanomaterials did not change to sorbed phases over time.

Figure 2 shows the XANES spectra for zinc sorbed to kaolin and the zinc oxide nanomaterial reacted with kaolin up to 12 months of aging. The spectra for Zn sorption (Figure 2A) show no changes during the aging process; however, zinc oxide undergoes extreme and rapid conversion during this time period in comparison to the unreacted ZnO nanomaterial (Figure 2B, top spectrum). Within 1 day, the shape and structure of the ZnO/kaolin XANES spectra transforms from ZnO to spectra similar to Zn sorbed on kaolin indicating a destabilization/dissolution of the ZnO nanoparticles with time (Figure 2B). The reaction conditions of the ZnO−kaolin system yield a negatively charged kaolin surface and a positively charged ZnO surface with potential electrostatic interaction of the materials. These conditions may allow sorption of the charged ZnO nanoparticles to the kaolin surface followed by destabilization/dissolution. This transformation was not evident for preliminary batch experiments of ZnO nanoparticles without kaolin at pH 6 and 0.01 M $NaNO_3$ aged to 3 months (data not shown) supporting the hypothesis that the kaolin surface is directly driving the

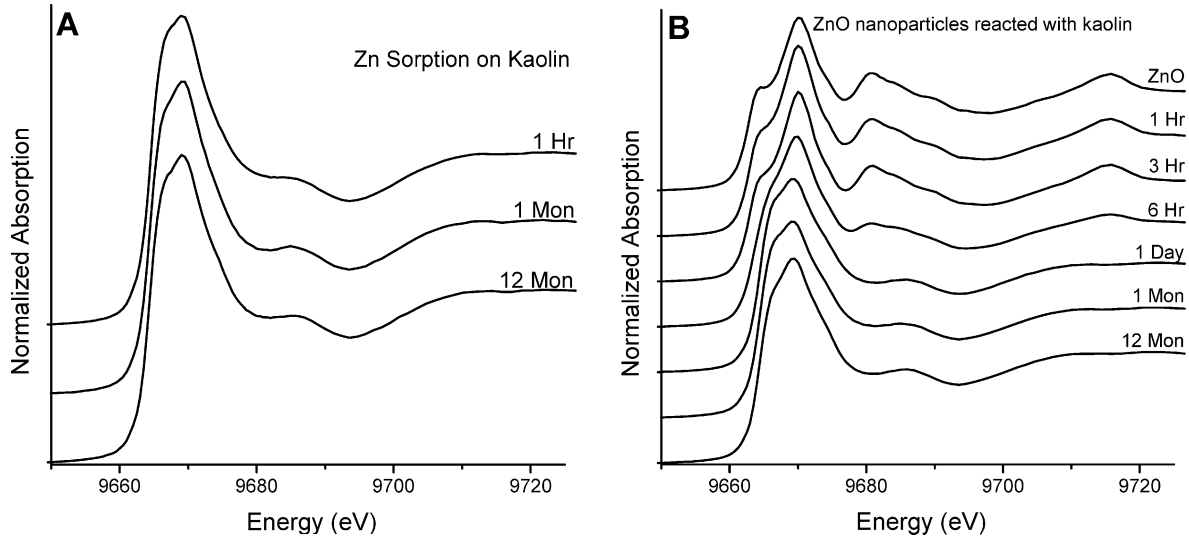

FIGURE 2. Zn−K_α XAS spectra (A) Zn sorbed on kaolin and (B) ZnO nanomaterial reacted with kaolin as a pure phase and reacted with kaolin as a function of aging. ZnO reacted with kaolin observed significant changes in Zn speciation over reaction times of 1 hour to 12 months.

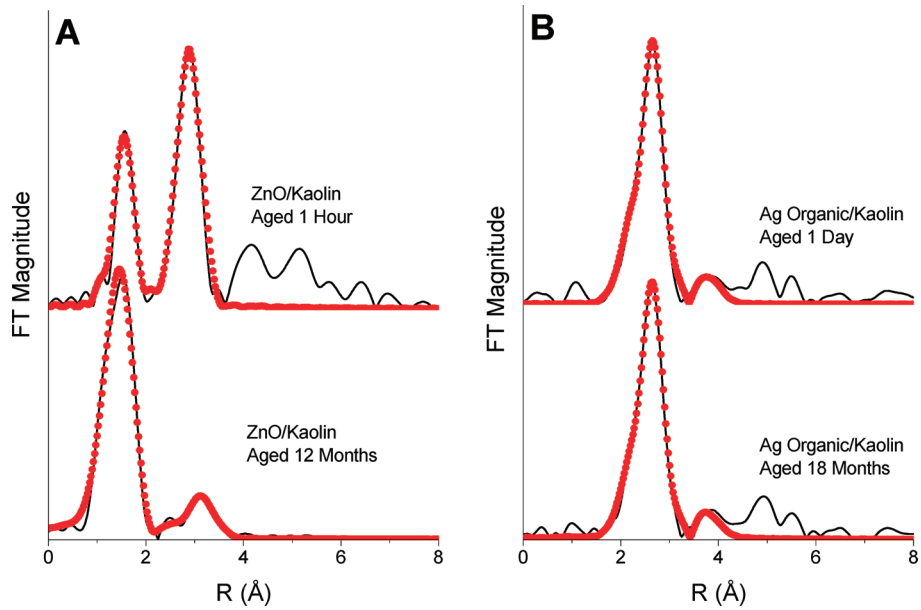

FIGURE 3. Measured (solid black lines) and fitted (dotted red lines) radial distribution functions of ZnO (A) and Ag Organic (B) nanomaterials reacted with kaolin in sodium nitrate as a function of aging time.

destabilization/dissolution of ZnO. The stability of aged ZnO nanoparticles in pure suspensions as a function of temperature, water content, and the presence of reaction products was observed by Meulenkamp (*36*) and noted rigid stability of the ZnO structure with analytical confirmation by XRD and UV/Vis spectroscopies. This highlights a key point for environmental scientists and toxicologists that soil and sediment environments may strongly influence the fate and stability of nanoparticles. Results of toxicological testing of nanomaterials in water or pure systems may not extrapolate to the natural environment where reactive surfaces and ligands are abundant. In fact, the behavior of ZnO nanomaterial in our kaolin system suggests that the environmental risk assessment should be more similar to Zn salts than stable ZnO nanoparticles in water.

Extended X-ray Absorption Fine Structure Spectroscopy. The radial distribution functions (RDFs) for Ag Organic and ZnO in 0.01 M $NaNO_3$ as a function of aging time are shown in Figure 3. The solid black lines are the measured data and the red dotted curves are the fitted data. The structural parameters from the EXAFS fitting are found in Table 2. The 1-hour reacted ZnO/kaolin sample shows two distinct peaks in the RDF representing Zn−O and Zn−Zn shells with coordination values of 4 and 12 and interatomic scattering distances of 1.97 Å and 3.22 Å, respectively, precisely matching the structural parameters for the ZnO standard material (Figure 3A, Table 2). As the ZnO/kaolin system aged to 12 months, the RDF appears significantly different than the 1 hour sample (Figure 3A). The fitting of the 12 month sample shows the presence of a Zn−O shell (CN, 6; *R*, 2.06 Å) and a Zn−Al shell (CN, 1.9; *R*, 3.10 Å) which are identical to Zn sorbed on the kaolin material (Table 2) and similar to Zn inner-sphere sorption complexes on kaolinite determined by others (*37*).

The conversion of ZnO to other Zn species in the environment has been previously studied. Voegelin et al. (*38*) examined soil samples containing between 2300 and 3900 mg kg^{-1} Zn as bulk ZnO from filter dust of a brass foundry over a 4 year period. At these elevated concentrations relative to our study, Voegelin et al. (*38*) found all of the ZnO was redistributed to Zn layered double hydroxide precipitates and Zn sorbed to organic matter or inorganic clay minerals within 9 months. The bioavailability of zinc as ZnO is significantly lower than aqueous Zn (*39*), but no data are available to address the bioavailability of sorbed Zn. However, a study comparing the release of Zn from ZnO containing tire debris, bulk ZnO, and sorbed Zn in amended soils was accomplished (*40*) and demonstrated sorbed Zn was more labile than ZnO and ZnO containing tire debris. In the case of ZnO nanoparticles converting to sorbed Zn phases upon aging in the environment, the increased availability of sorbed Zn may have an impact on ecoreceptors at elevated concentrations.

TABLE 2. Structural Parameters Derived from XAS Analysis

sample[f]	shell	CN[a]	*R*[b]	σ^2 [c]
ZnO, 1 hour	Zn−O	4	1.97	0.002
	Zn−Zn	12	3.22	0.007
ZnO, 12 months	Zn−O	6	2.06	0.004
	Zn−Al	1.9	3.10	0.006
ZnO standard	Zn−O	4	1.98	0.002
	Zn−Zn	12	3.21	0.004
Zn Sorbed kaolin	Zn−O	6.1	2.07	0.011
	Zn−Al	1.9	3.09	0.010
Ag Uncoated, 1 day	Ag−Ag	11.9	2.86	0.007
	Ag−Ag	6	4.09	0.010
Ag Uncoated, 18 months	Ag−Ag	12	2.87	0.008
	Ag−Ag	6	4.06	0.010
Ag Organic, 1 day	Ag−Ag	12	2.86	0.010
	Ag−Ag	6	4.07	0.010
Ag Organic, 18 months	Ag−Ag	12	2.86	0.008
	Ag−Ag	5.9	4.08	0.010
Ag Organic + NaCl, 12 months	$Ag-Cl_{Cl1}$[d]	5.9	2.78	0.005
	$Ag-Ag_{Ag1}$[e]	12	2.86	0.005
	$Ag-Ag_{Cl2}$	11.8	3.90	0.008
	$Ag-Ag_{Ag2}$	5.8	4.07	0.010
Ag metal	Ag−Ag	12	2.89	0.001
	Ag−Ag	6	4.09	0.003
AgCl	Ag−Cl	6	2.77	0.004
	Ag−Ag	12	3.92	0.004

[a] Coordination number [b] Interatomic bond distance [c] Debye -Waller factor [d] Fit path for AgCl [e] Fit path for Ag metal. [f] Samples are in bold, and reference materials are not bold.

The EXAFS fitting of Ag Organic (Figure 3B) for aging times of 1 day and 18 months identified two Ag−Ag shells with coordination numbers of about 12 and 6 and interatomic scattering distances of 2.86−2.87 Å for the first shell and

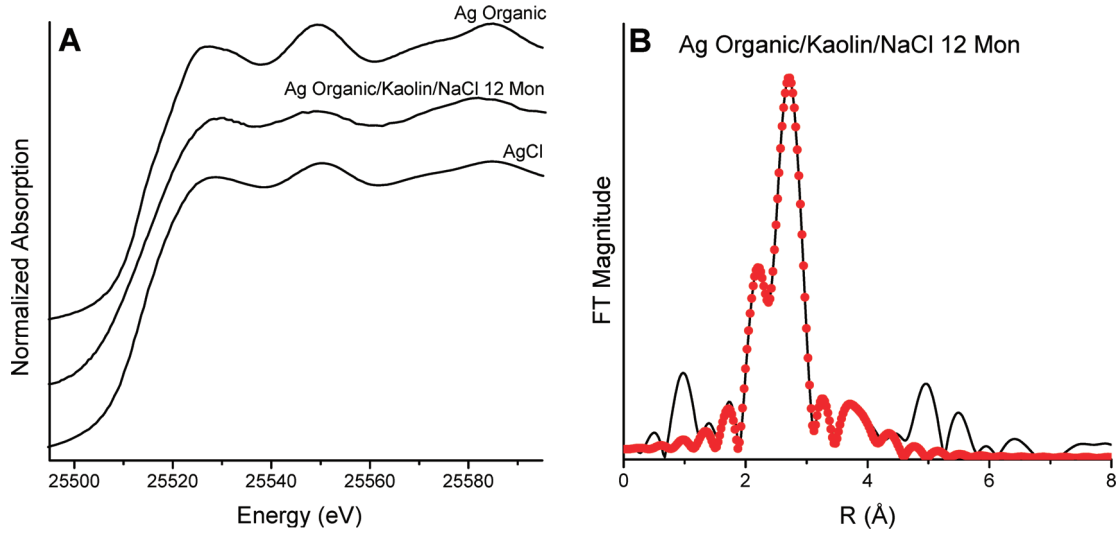

FIGURE 4. Ag−K_α XAS spectra (A) of Ag Organic nanoparticles and AgCl as pure phases, and Ag Organic reacted kaolin in 0.01 M NaCl aged for 12 months (left side) with (B) measured (solid black lines) and fitted (dotted red lines) radial distribution function showing the influence of chloride ion (right side).

4.06−4.09 Å for the second shell. Similar results were found for Ag Uncoated (Table 2) as well as other aging times for each nanomaterial that are not shown. These values confirm the presence of silver metal nanoparticles and that aging in the kaolin suspension with a sodium nitrate background electrolyte did not alter the speciation of the nanomaterial for aging times up to 18 months. The results indicate that potential antimicrobial features of metallic Ag nanoparticles may be retained in some environments that could influence exposure on microorganism populations.

However, alteration of the Ag Organic nanomaterial did occur when the sodium nitrate electrolyte was replaced with sodium chloride and aged up to 12 months (Figure 4). A very slow change was evident in the XANES spectra over time for Ag Organic in the kaolin suspension with 0.01 M NaCl resulting in a slight broadening of the white line peak (Figure 4A). EXAFS fitting of Ag Organic in the NaCl suspension aged for 12 months found the presence of both metallic silver and silver chloride (Figure 4B). Four fitting paths were used to explain the results (*41*). For the first shell ($\sim 2 < R < 3$ Å), a $Ag-Cl_{Cl1}$ bond for silver chloride was identified with a coordination value of 5.9 and bond distance of 2.78 Å and a $Ag-Ag_{Ag1}$ bond (Ag metal) yielded a coordination number of 12 and distance of 2.86 Å (Table 2). The second shell ($\sim 3 < R < 4.1$) was fitted as $Ag-Ag_{Cl2}$ and $Ag-Ag_{Ag2}$ with coordination values of 11.8 and 5.8, and interatomic scattering distances of 3.90 Å and 4.07 Å, respectively (Table 2). It is conceivable that silver chloride is coating the surface of the silver nanoparticles in situ as a common reaction pathway often observed when chloride and silver interact (*42*). Mono- and multilayer formation of silver chloride on metallic silver surfaces occur stepwise by Cl^- adsorption−desorption then nucleation−growth processes (*42*). The synchrotron beam at 25.5 KeV can easily pass through (attenuation depth of 100 μm for metallic silver and estimated 0.279 cm for kaolin at that energy) the 100 nm silver particles providing a signal for both silver chloride and metallic silver. The effect of speciation on the acute and chronic toxicity of silver has been studied extensively with conclusive evidence that silver chloride is approximately 300 times less toxic than silver ion (*43, 44*). A surface coating of silver chloride on silver nanoparticles may hinder the intended toxicological effects of the pure silver nanomaterial thus reducing harmful impacts on ecoreceptors in the environment. The formation of AgCl will also diminish the efficacy, over time, of Ag nanomaterials used as antimicrobial agents in consumer products (*45*) before they enter the environment.

Environmental Impact of Nanoparticle Aging. Chemical or physical changes to metal (oxide) nanoparticles as a result of aging in the environment may lead to reaction products that accumulate in soil and sediment profiles with significantly different toxicological effects. Chemical and physical transformations of manufactured nanoparticles released into the environment, either intentionally or inadvertently, must be studied in greater detail to gauge their long-term fate. There are many environmental factors that will govern the chemical and physical aspects of nanomaterials in the environment. Characterization, behavior, and deposition of nanoparticle aggregates in addition to speciation changes with aging will be important for risk assessment and management strategies. Alteration of nanoparticles in the environment adds complexity to risk assessment and decision support tools which often assume the nanomaterial of interest remains as a stable phase indefinitely. Identifying potential changes requires the use of advanced spectroscopic techniques and an understanding of colloidal chemistry. Additionally, results from aquatic toxicity tests, commonly used for environmental risk assessment, should be interpreted with caution as aging of the nanoparticles and the reactive media containing them could greatly influence the results (*16*).

Given the various manufactured nanomaterials employed in consumer products, the three examined in this study are a small part of a greater research need to evaluate nanoparticles in the environment. The impact of capping agents (surface coatings or functional groups), which can change the dynamics of nanomaterial surface chemistry and mobility, is another critical research need. Likewise, the intricacy of future studies that examine the influence of aging in environmental systems must examine the impact of a wider selection of reactive surfaces such as iron oxides and organic matter as well as broader reaction conditions including different pH and redox variables, which, for example, may impact metal sulfide nanoparticles. Regardless of the experimental conditions, evaluation of the long-term fate of nanoparticles in the environment must address the chemical and physical influence of aging to accurately predict stability and toxicity.

Acknowledgments

Any opinions expressed in this paper are those of the author(s) and do not, necessarily, reflect the official positions and policies of the USEPA. Any mention of products or trade names does not constitute recommendation for use by the

USEPA. MRCAT operations are supported by the Department of Energy and the MRCAT member institutions. We are grateful to Ms. Deborah Roose for ICP-OES analysis.

Literature Cited

(1) Ju-Nam, Y.; Lead, J. R. Manufactured nanoparticles: An overview of their chemistry, interactions and potential environmental implications. *Sci. Total Environ.* **2008**, *400* (1−3), 396–414.

(2) Klaine, S. J.; Alvarez, P. J. J.; Batley, G. E.; Fernandes, T. F.; Handy, R. D.; Lyon, D. Y.; Mahendra, S.; McLaughlin, M. J.; Lead, J. R. Nanomaterials in the environment: Behavior, fate, bioavailability, and effects. *Environ. Toxicol. Chem.* **2008**, *27* (9), 1825–1851.

(3) Li, Q.; Mahendra, S.; Lyon, D. Y.; Brunet, L.; Liga, M. V.; Li, D.; Alvarez, P. J. J. Antimicrobial nanomaterials for water disinfection and microbial control: Potential applications and implications. *Water Res.* **2008**, *42* (18), 4591–4602.

(4) Wiesner, M. R.; Lowry, G. V.; Alvarez, P.; Dionysiou, D.; Biswas, P. Assessing the risks of manufactured nanomaterials. *Environ. Sci. Technol.* **2006**, *40* (14), 4336–4345.

(5) Biswas, P.; Wu, C. Y. 2005 Critical Review: Nanoparticles and the environment. *J. Air Waste Manage.* **2005**, *55* (6), 708–746.

(6) Nowack, B.; Bucheli, T. D. Occurrence, behavior and effects of nanoparticles in the environment. *Environ. Pollut.* **2007**, *150* (1), 5–22.

(7) LowryG. V. CasmanE. A. Nanomaterial Transport, Transformation, and Fate in the Environment. In *Nanomaterials: Risks and Benefits*; Linkov, I., Steevens, J.; Springer: Dordrecht, The Netherlands, 2009; pp 125−137.

(8) Jiang, J. K.; Oberdorster, G.; Biswas, P. Characterization of size, surface charge, and agglomeration state of nanoparticle dispersions for toxicological studies. *J. Nanopart. Res.* **2009**, *11* (1), 77–89.

(9) Sarathy, V.; Tratnyek, P. G.; Nurmi, J. T.; Baer, D. R.; Amonette, J. E.; Chun, C. L.; Penn, R. L.; Reardon, E. J. Aging of iron nanoparticles in aqueous solution: Effects on structure and reactivity. *J. Phys. Chem. C* **2008**, *112* (7), 2286–2293.

(10) Tombacz, E.; Illes, E.; Majzik, A.; Hajdu, A.; Rideg, N.; Szekeres, M. Ageing in the inorganic nanoworld: Example of magnetite nanoparticles in aqueous medium. *Croat. Chem. Acta* **2007**, *80* (3−4), 503–515.

(11) Klausen, J.; Vikesland, P. J.; Kohn, T.; Burris, D. R.; Ball, W. P.; Roberts, A. L. Longevity of granular iron in groundwater treatment processes: Solution composition effects on reduction of organohalides and nitroaromatic compounds. *Environ. Sci. Technol.* **2003**, *37* (6), 1208–1218.

(12) Schrick, B.; Blough, J. L.; Jones, A. D.; Mallouk, T. E. Hydrodechlorination of trichloroethylene to hydrocarbons using bimetallic nickel-iron nanoparticles. *Chem. Mater.* **2002**, *14* (12), 5140–5147.

(13) Sohn, K.; Kang, S. W.; Ahn, S.; Woo, M.; Yang, S. K. Fe(0) nanoparticles for nitrate reduction: Stability, reactivity, and transformation. *Environ. Sci. Technol.* **2006**, *40* (17), 5514–5519.

(14) Liu, Y. Q.; Lowry, G. V. Effect of particle age (Fe^0 content) and solution pH on NZVI reactivity: H_2 evolution and TCE dechlorination. *Environ. Sci. Technol.* **2006**, *40* (19), 6085–6090.

(15) Scheckel, K. G.; Chaney, R. L.; Basta, N. T.; Ryan, J. A. Advances in assessing bioavailability of metal(loid)s in contaminated soils. *Adv. Agron.* **2009**, *104*, 1–52.

(16) Phenrat, T.; Long, T. C.; Lowry, G. V.; Veronesi, B. Partial oxidation ("aging") and surface modification decrease the toxicity of nanosized zerovalent iron. *Environ. Sci. Technol.* **2009**, *43* (1), 195–200.

(17) Adams, L. K.; Lyon, D. Y.; Alvarez, P. J. J. Comparative ecotoxicity of nanoscale TiO_2, SiO_2, and ZnO water suspensions. *Water Res.* **2006**, *40* (19), 3527–3532.

(18) Dawson, T. L. Nanomaterials for textile processing and photonic applications. *Color. Technol.* **2008**, *124* (5), 261–272.

(19) Blaise, C.; Gagne, F.; Ferard, J. F.; Eullaffroy, P. Ecotoxicity of selected nano-materials to aquatic organisms. *Environ. Toxicol.* **2008**, *23* (5), 591–598.

(20) Blaser, S. A.; Scheringer, M.; MacLeod, M.; Hungerbuhler, K. Estimation of cumulative aquatic exposure and risk due to silver: Contribution of nano-functionalized plastics and textiles. *Sci. Total Environ.* **2008**, *390* (2−3), 396–409.

(21) Franklin, N. M.; Rogers, N. J.; Apte, S. C.; Batley, G. E.; Gadd, G. E.; Casey, P. S. Comparative toxicity of nanoparticulate ZnO, bulk ZnO, and $ZnCl_2$ to a freshwater microalga (*Pseudokirchneriella subcapitata*): The importance of particle solubility. *Environ. Sci. Technol.* **2007**, *41* (24), 8484–8490.

(22) Griffitt, R. J.; Luo, J.; Gao, J.; Bonzongo, J. C.; Barber, D. S. Effects of particle composition and species on toxicity of metallic nanomaterials in aquatic organisms. *Environ. Toxicol. Chem.* **2008**, *27* (9), 1972–1978.

(23) Wiench, K.; Wohlleben, W.; Hisgen, V.; Radke, K.; Salinas, E.; Zok, S.; Landsiedel, R. Acute and chronic effects of nano- and non-nano-scale TiO_2 and ZnO particles on mobility and reproduction of the freshwater invertebrate Daphnia magna. *Chemosphere* **2009**, *76* (10), 1356–1365.

(24) Sparks, D. L., *Environmental Soil Chemistry*; Academic Press, Inc.: San Diego, CA, 1995.

(25) Sparks, D. L. *Methods of Soil Analysis: Chemical Methods*,Book Series No. 5; Soil Science Society of America: Madison, WI 1996.

(26) Abdelwaheda, W.; Degoberta, G.; Stainmesseb, S.; Fessi, H. Freeze-drying of nanoparticles: Formulation, process and storage considerations. *Adv. Drug Deliver. Rev.* **2006**, *58* (15), 1688–1713.

(27) Ravel, B.; Newville, M. ATHENA, ARTEMIS, HEPHAESTUS: data analysis for X-ray absorption spectroscopy using IFEFFIT. *J. Synchrotron Rad.* **2005**, *12* (4), 537–541.

(28) Ressler, T. WinXAS: A program for X-ray absorption spectroscopy data analysis under MS-Windows. *J. Synchrotron Rad.* **1998**, *5*, 118–122.

(29) Newville, M.; Livicnvs, P.; Yacoby, Y.; Rehr, J. J.; Stern, E. A. Near-edge x-ray-absorption fine structure of Pb: A comparison of theory and experiment. *Phys. Rev. B* **1993**, *47* (21), 14126–14131.

(30) Antelmi, D. A.; Spalla, O. Adsorption of nanolatex particles to mineral surfaces of variable surface charge. *Langmuir* **1999**, *15* (22), 7478–7489.

(31) Weng; Van Riemsdijk, W. H.; Hiemstra, T. Adsorption free energy of variable-charge nanoparticles to a charged surface in relation to the change of the average chemical state of the particles. *Langmuir* **2005**, *22* (1), 389–397.

(32) Altin, O.; Ozbelge, H. O.; Dogu, T. Use of general purpose adsorption isotherms for heavy metal-clay mineral interactions. *J. Colloid Interface Sci.* **1998**, *198* (1), 130–140.

(33) Bolt, G. H.; De Boodt, M. F.; Hayes, H. B.; McBride, M. B., *Interactions at the Soil Colloid-Soil Solution Interface*; Kluwer Academic Publishers: Netherlands, 1991; Vol. 190, p 603.

(34) Cop, A.; Kovacevic, D.; Dragic, T.; Kallay, N. Evaluation of equilibrium parameters characterizing metal oxide/electrolyte solution interface. *Colloid Surf. A.* **2004**, *230* (1−3), 159–165.

(35) Hill, D. M.; Aplin, A. C. Role of colloids and fine particles in the transport of metals in rivers draining carbonate and silicate terrains. *Limnol. Oceanogr.* **2001**, *46* (2), 331–344.

(36) Meulenkamp, E. A. Synthesis and growth of ZnO Nanoparticles. *J. Phys. Chem. B.* **1998**, *102*, 5566–5572.

(37) Nachtegaal, M. M.; Sparks, D. L. Effect of iron oxide coatings on zinc sorption mechanisms at the clay-mineral/water interface. *J. Colloid Interface Sci.* **2004**, *276*, 13–23.

(38) Voegelin, A.; Pfister, S.; Scheinost, A. C.; Marcus, M. A.; Kretzschmar, R. Changes in zinc speciation in field soil after contamination with zinc oxide. *Environ. Sci. Technol.* **2005**, *39* (17), 6616–6623.

(39) Wedekind, K. J.; Lewis, A. J.; Giesemann, M. A.; Miller, P. S. Bioavailability of zinc from inorganic and organic sources for pigs fed corn-soybean meal diets. *J. Anim. Sci.* **1994**, *72* (10), 2681–2689.

(40) Smolders, E.; Degryse, F. Fate and effect of zinc from tire debris in soil. *Environ. Sci. Technol.* **2002**, *36* (17), 3706–3710.

(41) Kelly, S.; Hesterberg, D.; Ravel, B. , Analysis of soils and minerals using X-ray absorption spectroscopy. In *Methods of Soil Analysis. Part 5. Mineralogical Methods*; Ulery, A. L.; Drees, L. R. , Eds.; Soil Science Society of America: Madison, WI, 2008; pp 387−463.

(42) Jaya, S.; Rao, T. P.; Rao, G. P. Mono-and multilayer formation studies of silver chloride on silver electrodes from chloride-containing solutions. *J. Appl. Electrochem.* **1987**, *17* (3), 635–640.

(43) Kegley, S. E.; Hill, B. R.; Orme, S.; Choi, A. H. PAN Pesticides Database—Chemicals. http://www.pesticideinfo.org/.

(44) USEPA Integrated Risk Information System (IRIS). http://www.epa.gov/iris/.

(45) Impellitteri, C. A.; Tolaymat, T. M.; Scheckel, K. G. The speciation of silver nanoparticles in antimicrobial fabric before and after exposure to a hypochlorite/detergent solution. *J. Environ. Qual.* **2009**, *38* (4), 1528–1530.

ES9032265